Physica Scripta. Vol. T118, 165–167, 2005

Effects of Lattice Structure in the Dynamics of Coupled Elements

André S. Ribeiro[1] and Pedro G. Lind[2,3*]

[1]Department of cell biology and physiology, University of New Mexico, 87131-0001, USA. Centre for computational physics, University Coimbra, P-3004-516 Coimbra, Portugal
[2]Institut für Computer Anwendungen, Universität Stuttgart, Pfaffenwaldring 27, D-70569 Stuttgart, Germany
[3]Centro de Física Teórica e Computacional, Av. Prof. Gama Pinto 2, 1649-003 Lisbon, Portugal

Received October 18, 2003; revised version received July 14, 2004; accepted August 6, 2004

PACS numbers: 89.75.Kd, 05.45.−a, 05.45.Xt, 02.10.Ox

Abstract

We investigate the influence of lattice geometry in network dynamics, using a cellular automaton with nearest-neighbor interactions and two admissible local states. We show that there are significant geometric effects in the distribution of local states and in the distribution of clusters, even when the connection topology is kept constant. Moreover, we show that some geometric structures are more cohesive than others, tending to keep a given initial configuration. To characterize the dynamics, we determine the distributions of local states and introduce a cluster coefficient. The lattice geometry is defined from the number of nearest neighbors and their disposition in 'space', and here we consider four different geometries: a chain, a hexagonal lattice, a square lattice and a cubic lattice.

1. Introduction

Recently, networks of coupled elements have been successfully applied to model particular dynamical features of physical systems such as lasers [1], electric circuits [2], connected oscillators [3], and many others [4, 5]. In general, underlying these networks there is some characteristic connection topology [6], which is defined essentially by [7] the average path length $\langle \ell \rangle$, i.e. the average of the shortest path (number of connections) between all pairs of nodes, and the clustering coefficient which measures the fraction of effective connections between the neighbors of some fixed site out from the total number of possible connections.

One of the most famous models studied with the help of these two quantities is the so-call small-world model [7, 8, 9, 10], where one considers networks ranging from regular to random connections between the elements (nodes). These middle ground topologies are characterized by large values of the clustering coefficient and simultaneously by small average path lengths. For completely regular lattices, both quantities are in fact related [9, 10]: the average path length $\langle \ell \rangle$ measures the velocity of signal propagation through the lattice, and decreases when the number of connections increases.

In the particular case of homogeneous connections, i.e. all pairs of connected nodes are connected with the same strength, it is possible to associate some specific spatial geometric structure. For instance, if each node is connected to two and only two other nodes, one may think in a chain of nodes with nearest neighbors connections; if, instead of two, one has four and only four connections for each node, the network is 'homeomorphic' to a square lattice.

Spatial structure and geometry of lattice systems play a fundamental role in the dynamics underlying physical and complex systems. For instance, it was recently found [11] that metastable structures of lattices of single-wall carbon nanotubes depend strongly on the geometric polygon defining their tube cross sections. Moreover, in spatially extended systems geometric effects are of fundamental importance, e.g. in the stability of crystal lattices of two-dimensional superparamagnetic suspensions [12], in the temperature evolution of molecular structures [13], in tree networks with causal structure [14], and even in nonlinear collective effects of Bose-Einstein condensates in optical lattices [15].

The aim of this paper is to consider periodic lattice structures all of them with the same topological characteristics, average path length and clustering coefficient, and investigate what differences prevail in their dynamics when only the lattice geometry is varied.

To this end, we choose four different lattice geometries with k nearest neighbors, a chain ($k = 2$), a hexagonal lattice ($k = 3$), a square lattice ($k = 4$) and a cubic lattice ($k = 6$), and impose a dynamical framework defined by a cellular automaton as a prototype model of dynamical systems with spatiotemporal complexity. Cellular automata have been recently used in physical systems [16], for instance to perform clocked logic operations on discrete particles in nanostructured superconducting geometries [17], and also to study biologic phenomena, such the evolution of self-replicating molecules [18] and tumors growth [19]. In particular, two-state cellular automata are used for example as alternative models of quantum computation [20], to model traffic flow [21, 22], and to optimize traffic lights in nets of city streets [23, 24].

Here, we also consider a two-state cellular automaton, whose local states $s = 0$ and $s = 1$ evolve according to a nearest-neighbor homogeneous coupling: for each node $\boldsymbol{r}$ the present state $s_t(\boldsymbol{r})$ influences with the same weight the future state $s_{t+1}(\boldsymbol{r})$ as its neighborhood, and the neighborhood contributes to that future state as a mean field of the k nearest neighbors. In other words, the equation of evolution for our model reads

$$s_{t+1}(\boldsymbol{r}) = \mathcal{H}(S_t(\boldsymbol{r}) - 1), \tag{1}$$

where $\mathcal{H}(x)$ is the Heaviside function, guaranteeing that $s_{t+1}(\boldsymbol{r})$ assumes only the values 0 and 1, and the quantity $S_t(\boldsymbol{r})$, which varies between 0 and 2, is given by

$$S_t(\boldsymbol{r}) = s_t(\boldsymbol{r}) + \frac{1}{k} \sum_{\boldsymbol{r}',k} s_t(\boldsymbol{r}'), \tag{2}$$

with $\boldsymbol{r}'$ representing the coordinates of the k nearest neighbors. From Eqs. (1) and (2), one easily sees that each future local state tends to be at the same state as the majority part of the sites $\boldsymbol{r}$ and $\boldsymbol{r}'$. The particular case $S_t(\boldsymbol{r}) = 1$, for which $s_{t+1}(\boldsymbol{r}')$ has a discontinuity, occurs only when all neighbors of node $\boldsymbol{r}$ are at the same state, different from the state of node $\boldsymbol{r}$, and, in this case, we assume that $\boldsymbol{r}$ changes to the state of its neighbors.

*Corresponding author: lind@ical.uni-stuttgart.de

This model has the property that, for any geometry, i.e. for any value of k, the number of combinations of local states and neighboring states evolving toward a future state $s_{t+1}(\boldsymbol{r}) = 0$ equals the number of combinations evolving toward $s_{t+1}(\boldsymbol{r}) = 1$. Moreover, for $k = 2$, i.e. in the case of one-dimensional cellular automaton with nearest-neighboring coupling, the model in Eq. (1) reduces to the Wolfram's rule number 232 (see Ref. [16]). Here, we choose periodic boundary conditions.

With this framework and fixing the average path length and the clustering coefficient one guarantees that all differences in the dynamics are due to the lattice geometry, i.e. to the 'disposition' of nodes in space. Therefore, in the next Section 2 we describe how to fix these topological quantities for all lattice geometries and introduce two dynamical quantities from which one is able to compare the geometric effects in local states dynamics. Conclusions are summarized in Section 3.

2. Comparing different lattice geometries

In this Section we study state and cluster distributions for each lattice geometry mentioned above, considering the cellular automaton ruled by Eq. (1). More precisely, we determine the fraction R_s of states at $s = 0$ and measure a cluster coefficient R_c which quantifies the tendency for cluster formation. Here, we use the usual definition of cluster [4, 5], i.e. a set of adjacent nodes at the same state, and therefore, the cluster coefficient R_c is defined from the fraction of adjacent nodes at different states, namely

$$R_c = 1 - \frac{1}{kN} \sum_{\boldsymbol{r},N} \sum_{\boldsymbol{r}',k} |S_t(\boldsymbol{r}) - S_t(\boldsymbol{r}')|. \tag{3}$$

As one sees from Eq. (3), the cluster coefficient ranges from 0, when any two adjacent nodes have different amplitudes, i.e. the number of clusters equals the number of nodes, and 1, when all nodes have the same amplitude, i.e. the entire lattice is composed by a single cluster.

For each lattice geometry Table I gives an exact expression of the average path length $\langle \ell \rangle$ as a function of the total number N of nodes. These expressions are obtained either from the corresponding adjacency matrix or from geometric procedures, and the complete deduction will be presented elsewhere. For all the four geometries the clustering coefficient is always 0. Therefore, to impose the same value of the topological quantities one just needs to determine the number of nodes in each case, namely for the chain of nodes we choose $N = 143$, for the hexagonal lattice $N = 12$, for the square lattice $N = 72$, and for the cubic lattice $N = 48$. For these choices one finds approximately the same average path length, namely $\langle \ell \rangle = 36$ for both the chain and the hexagonal lattice, $\langle \ell \rangle = 36.0069$ for the square lattice and $\langle \ell \rangle = 36.0007$ for the cubic lattice.

Table I. *The average path length $\langle \ell \rangle$ for four different geometric structures with k nearest neighbors: a chain ($k = 2$), a hexagonal lattice ($k = 3$), a square lattice ($k = 4$), and a cubic lattice ($k = 6$). See appendix I for details.*

Geometry	Chain ($k = 2$)	Hexagonal ($k = 3$)	Square ($k = 4$)	Cubic ($k = 6$)
$\langle \ell \rangle_k$	$\frac{N+1}{4}$ (n odd) $\frac{N^2}{4(N-1)}$ (n even)	$\frac{7}{12}N^{3/2} - \frac{1}{3}N^{1/2}$	$\frac{\sqrt{N}}{2}$ (n odd) $\frac{N^{3/2}}{2(N-1)}$ (n even)	$\frac{3(N+N^{2/3})}{4(N^{2/3}+N^{1/3}+1)}$ (n odd) $\frac{3(N^{4/3}+N^{1/3})}{4(N-1)}$ (n even)

Figure 1a shows for each geometry the distribution F of fraction R_s of states at $s = 0$, from a sample of 10^6 random initial configurations, while Fig. 1b shows the same distribution after a transient of 10^3 time-steps, beyond which the system is thermalized. While for $k = 2$ the unit interval where fraction R_s is defined was divided always in 100 subintervals, for the other geometries the number of divisions depends on the total number N of nodes. Therefore, although the four distributions have apparently different 'integrals', they are in fact all equal to 1.

From Fig. 1a one clearly observes Gaussian distributions of the initial configurations, centered at $R_s = 0.5$, whose widths ω_s^0 depend on the geometry, decreasing when k increases. After thermalization (Fig. 1b), one observes that all distributions remain centered at $R_s = 0.5$, but now they have a different width ω_s then the initial one. Since the width of the distribution of initial random configurations depends on the total number N of nodes used for each geometry, to compare geometric effects in the final state distribution, one must compare the ratio ω_s/ω_s^0. Here, one finds $\omega_s/\omega_s^0 \sim 3.4$ for the chain, $\omega_s/\omega_s^0 \sim 2.6$ for the hexagonal lattice, $\omega_s/\omega_s^0 \sim 2.1$ for the square lattice and $\omega_s/\omega_s^0 \sim 0.8$ for the cubic lattice. Therefore, from these values, one clearly sees that different geometries correspond to different state distributions.

Figure 1c displays the distributions of the clustering coefficient R_c for the same sample of initial configurations, after thermalization, while in the inset one shows the corresponding initial distributions of R_c. The main point here is that when changing the geometry, one observes a distribution of R_c not only with a different width, but also with a different mean value μ_c. In fact, after thermalization the mean values are quite different: $\mu_c = 0.84$ for the chain, $\mu_c = 0.78$ for the hexagonal lattice, $\mu_c = 0.61$ for the square lattice and $\mu_c = 0.54$ for the cubic lattice. In other words, the mean value of cluster distributions decreases when the number of k nearest neighbors increase. Subtracting from this final mean μ_c the mean value μ_c^0 of the corresponding initial distribution, one finds a measure of the 'cohesion' in the system, i.e. a measure of the more or less ability of the system to change a given initial state configuration. In this sense, one concludes from Fig. 1c that the cubic lattice is the most cohesive one, while the chain allows more variation of state configurations with respect to some initial configuration from which the system evolves.

The particular feature observed for the chain ($k = 2$), whose cluster distribution has zero and non-zero values, is due to the fact that for this geometry $N \times R_c$ must be an even number. In fact, in the chain the product $N \times R_c$ equals precisely the number of clusters in the lattice and, since one has only two admissible local states, the number of clusters must be even. For all other geometries, R_c varies monotonically with the number of clusters, being still a suitable measure of the number of clusters and consequently a suitable measure of their average size.

All the results shown in Fig. 1 were obtained for a specific average path length $\langle \ell \rangle$. In Fig. 2 we show how the width ratios ω_s/ω_s^0 and ω_c/ω_c^0 and the mean difference $\mu_c - \mu_c^0$ vary with the average path length. Horizontal lines indicate the linear fitting obtained for each geometry. These fittings correspond to completely different values, depending on the geometry one is considering. Notice that, this fitting was computed from a wider spectrum of $\langle \ell \rangle$ then the one shown in the figure. Therefore, for the hexagonal lattice ($k = 3$), since average path length increases very fast with N, only one data point is visible in the range shown.

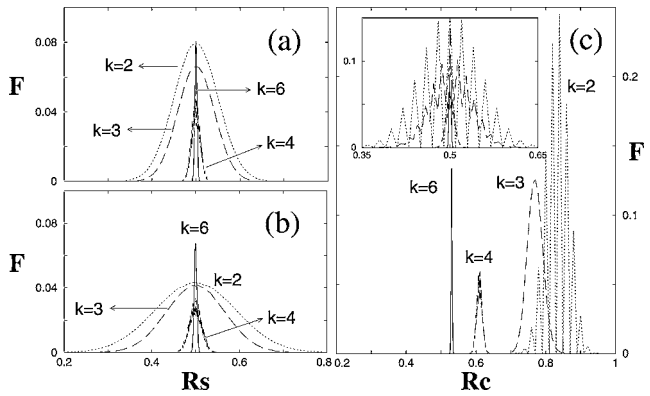

Fig. 1. Different lattice geometries have different widths of the distribution $F(R_s)$, where R_s is the fraction of states at $s = 0$. For each geometry one sees (**a**) the distribution $F(R_s)$ of a sample of 10^6 initial configurations and (**b**) the same distribution after a transient of 10^3 time-steps beyond which the system is thermalized. The ratio ω_s/ω_s^0 of both distribution widths, before and after thermalization, depends on the lattice geometry, i.e. on the value of k (see text). While the mean value of distributions $F(R_s)$ is always $\mu_s = 0.5$, (**c**) the distribution $F(R_c)$ of the cluster coefficient R_c, Eq. (3), shows a 'shifting' of the mean values when compared to the one of the initial configurations, shown in the inset ($\mu_c^0 = 0.5$).

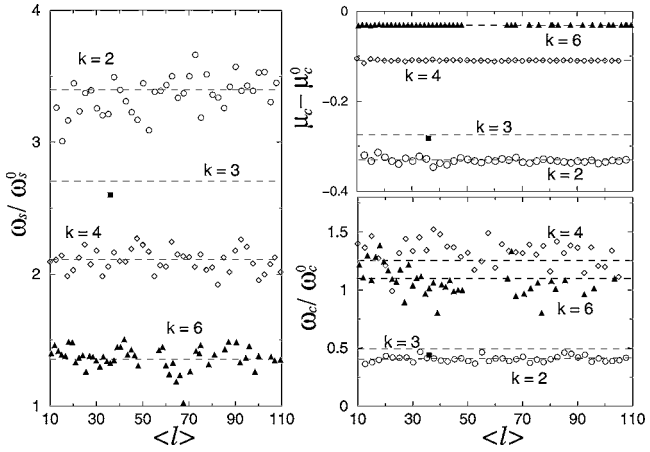

Fig. 2. **Left:** The ratio ω_s/ω_s^0 between the widths of final and initial state configurations distributions as a function of the average path length $\langle \ell \rangle$. **Right:** The ratio ω_c/ω_c^0 and the mean difference $\mu_c - \mu_c^0$ of the cluster distribution $F(R_c)$. All these quantities allow to distinguish between the four geometries (see text). Horizontal dashed lines indicate the linear fitting for each geometry, whose value characterizes each geometry.

As one clearly sees from Fig. 2, each geometry has specific values of the width ratios and mean differences. In fact although these quantities vary significantly with the average path length, oscillating around the horizontal fitting lines, for each geometry these variations occur in particular ranges of values. Therefore, lattice structure is well characterized by any of these quantities.

3. Conclusions

The purpose of this manuscript was to characterize lattice structures from their dynamical properties of collective motion. Here, we studied the influence of geometric structures in the dynamics of discrete systems, namely of a cellular automaton with two local states. Four different regular geometries were considered, namely a chain of nodes, a hexagonal lattice, a square lattice and a cubic lattice, each one having an appropriate number of nodes in order to impose some fixed average path length.

We found that the ratio between the width of the final state distribution and the width of the corresponding set of initial configurations characterizes each geometry. Moreover, we introduced a suitable cluster coefficient, which gives a measure of the number of clusters in the system, and found that even for a constant average path length, some geometries show more tendency to form clusters than other. In particular, the ability for cluster formation decreases significantly with the number of nearest neighbors.

For simplicity, we only investigated two-state cellular automaton. However, all the dynamical quantities, state distribution and cluster coefficient, can be easily extended to any spatially discrete extended systems. Moreover, since the lattice evolution depends only on the connections between elements (coupling topology) and not on specific functions (maps) of local states, we believe that for other cellular automata the geometric effects here reported should prevail.

As a final remark, from this preliminary study it would be interesting to investigate for each particular geometry, not only the number and the size of clusters emerging in the system, but also their shape and dynamics. These points are being studied and will be presented elsewhere.

Acknowledgments

The authors thank *Fundaço para a Cîncia e a Tecnologia*, Portugal, for two doctoral fellowships.

References

1. Uchida, A., Matsuura, T., Kinugawa, S. and Yoshimori, S., Phys. Rev. E **65**, 066212 (2002).
2. Smirnov, D. A., Bezruchko, B. P. and Seleznev, Y. P., Phys. Rev. E **65**, 026205 (2002).
3. Barahona, M. and Pecora, L., Phys. Rev. Lett. **89**, 054101 (2002).
4. Pikovsky, A., Rosenblum, M. and Kurths, J., "Synchronization – A Universal Concept in Nonlinear Sciences", (Cambridge University Press, Cambridge, 2001).
5. Boccaletti, S., Kurths, J., Osipov, G., Valladares, D. L. and Zhou, C. S., Phys. Reports **366**, 1 (2002).
6. Lind, P. G., Corte-Real, J. and Gallas, J. A. C., Phys. Rev. E **69**, 026209 (2004).
7. Watts, D. J. and Strogatz, D. H., Nature **393**, 440 (1998).
8. Strogatz, D. H., Nature **410**, 268 (2001).
9. Strogatz, S., "Sync: The Emerging Science of Spontaneous Order", (Hyperion, New York, 2003).
10. Albert, R. and Barabási, A.-L., Rev. Mod. Phys. **74**, 47 (2002).
11. López, M. J., Rubio, A., Alonso, J. A., Qin, L.-C. and Iijima, S., Phys. Rev. Lett. **86**, 3056 (2001).
12. Froltsov, V. A., Blaak, R., Likos, C. N. and Löwen, H. Phys. Rev. E **68**, 061406 (2003).
13. Fokin, A. V. *et al.*, Phys. Rev. Lett. **89**, 175503 (2002).
14. Bialas, P., Burda, Z., Jurkiewicz, J. and Krzywicki, A., Phys. Rev. E **67**, 066106 (2003).
15. Sukhorukov, A. A. and Kivshar, Y. S., Phys. Rev. Lett. **91**, 113902 (2003).
16. Wolfram, S., Rev. Mod. Phys. **55**, 601 (1983); "A New Kind of Science" (Wolfram Media Inc., New York, 2002).
17. Hastings, M. B., Olson Reichhardt, C. J. and Reichhardt, C., Phys. Rev. Lett. **90**, 247004 (2003).
18. Rosas, A., Ferreira, C. P. and Fontanari, J. F., Phys. Rev. Lett. **89**, 188101 (2002).
19. Galam, S. and Radomski, J. P., Phys. Rev. E **63**, 051907 (2001).
20. Brennen, G. K. and Williams, J. E., Phys. Rev. A **68**, 042311 (2003).
21. Yokoya, Y., Phys. Rev. E **69**, 016121 (2004).
22. Barlovic, R., Huisinga, T., Schadschneider, A. and Schreckenberg, M., Phys. Rev. E **66**, 046113 (2002).
23. Benyoussef, A., Chakib, H. and Ez-Zahraouy, H., Phys. Rev. E **68**, 026129 (2003).
24. Brockfeld, E., Barlovic, R., Schadschneider, A. and Schreckenberg, M., Phys. Rev. E **64**, 056132 (2001).

